Available online at www.sciencedirect.com

ScienceDirect

www.elsevier.com/locate/jes

JES JOURNAL OF ENVIRONMENTAL SCIENCES

www.jesc.ac.cn

Effect of NOx and RH on the secondary organic aerosol formation from toluene photooxidation☆

Shijie Liu[1], *Xiaodi Liu*[1], *Yiqian Wang*[1], *Si Zhang*[1], *Can Wu*[1], *Wei Du*[1], *Gehui Wang*[1,2,*]

[1] *Key Lab of Geographic Information Science of the Ministry of Education, School of Geographic Sciences, East China Normal University, Shanghai 210062, China*

[2] *Institute of Eco-Chongming, 3663 North Zhongshan Road, Shanghai 200062, China*

ARTICLE INFO

Article history:
Received 31 May 2021
Revised 11 June 2021
Accepted 16 June 2021
Available online 16 January 2022

Keywords:
Toluene
Photooxidation
Relative humidity
NOx
Optical property

ABSTRACT

The secondary organic aerosol (SOA) formation mechanism and physicochemical properties can highly be influenced by relative humidity (RH) and NOx concentration. In this study, we performed a laboratory investigation of the SOA formation from toluene/OH photooxidation system in the presence or absence of NOx in dry and wet conditions. The chemical composition of toluene-derived SOA was measured using Aerodyne high-resolution time-of-flight aerosol mass spectrometer (HR-ToF-AMS). It was found that the mass concentration of toluene decreased with increasing RH and NOx concentration. However, the change of SOA chemistry composition (f_{44}, O/C) with increased RH was not consistent in the condition with or without NOx. The light absorption and mass absorption coefficient (MAC) of the toluene-derived SOA only increased with RH in the presence of NOx. In contrast, MAC is invariant with RH in the absence of NOx. HR-ToF-AMS results showed that, in the presence of NOx, the increased nitro-aromatic compounds and N/C ratio concurrently caused the increase of SOA light absorption and O/C in wet conditions, respectively. The relative intensity of CHON and CHO_xN family to the total nitrogen-containing organic compounds (NOCs) increased with the increasing RH, and be the major components of NOCs in wet condition. This work revealed a synergy effect of NOx and RH on SOA formation from toluene photooxidation.

Introduction

Aromatic hydrocarbon compounds are widely emitted from anthropogenic sources (Han et al., 2021; Mehra et al., 2020; George et al., 2015), and their gas-phase oxidation reactions with OH are the most important processes in the atmosphere (Chen et al., 2021; Jia and Xu, 2018). Oxidation products with sufficiently low vapour pressure would transform into the particle-phase through nucleation and condensation, and term the secondary organic aerosol (SOA) (Ziemann and Atkinson, 2012; Zhang et al., 2019; Liu et al., 2019a; Carlton et al., 2009). SOA, as an important component of atmospheric particulate matter (PM), has a substantial impact on air quality and public human health (Chen et al., 2021;

☆ This article is dedicated to Professor Dianxun Wang.

* Corresponding author.
E-mail: ghwang@geo.ecnu.edu.cn (G. Wang).

https://doi.org/10.1016/j.jes.2021.06.017
1001-0742/

Zhang et al., 2015; Paciga et al., 2014). A kind of SOA with gradually increasing absorption spectrum from visible light to ultraviolet (UV) light could significantly impact the earth's radiation balance, influence the photochemical processes and cycles in the atmosphere (Liu et al., 2015a; Jo et al., 2016; Laskin et al., 2015), and resulted in the diversification of region climate (Moise et al., 2015). Recently, the optical property of SOA has been drawing more and more attentions.

SOA is a highly complex and dynamically mixed organic matter because of its complex primary sources and secondary formation processes. NOx is one of the most common pollutants in the atmospheric environment, and plays an important role in SOA formation (Schwantes et al., 2019; Priestley et al., 2021). NOx concentration not only closely relates to the concentrations of main atmospheric oxidants (like OH, NO_3 radicals and O_3), but also governs the competitive chemistry of peroxy radicals (RO_2) in the photooxidation process of VOCs (Schwantes et al., 2019; Zhao et al., 2018). Higher NOx concentration can suppress SOA formation as reduction of RO_2 to alkoxy radicals (RO) ultimately leads to fragmentation of the RO species (Sarrafzadeh et al., 2016; Surratt et al., 2006). The presence of NOx can also alter the chemical composition of SOA (Pullinen et al., 2020). Wang et al. (2019) reported that the oxidation of toluene and benzene in the presence of NOx was the dominant source of Nitrogen-containing organic compounds (NOCs), and the NOx concentration was an important factor influencing the secondary formation of NOCs (Wang et al., 2019). Multiple laboratory experiments and field studies have demonstrated that NOCs are the key components causing the increase of aerosol optical property (Chow et al., 2016; Lin et al., 2015; Liu et al., 2015b; Liu et al., 2019b). Xie et al. (2017) identified and quantified Fifteen NOCs chemical formulas from eight aromatic VOCs precursors in the presence of NOx, and pointed that the average contributions of these fifteen NOCs were two times greater than the average mass contributions of SOA to total light absorption (Xie et al., 2017).

In the troposphere, relative humidity (RH) is one of the most significant physical parameters that affect the SOA formation and photooxidation process. Many previous studies have investigated the effect of RH on SOA formation from VOCs (Jia and Xu, 2018; Chen et al., 2021; Liu et al., 2019a). The increased RH could increase the liquid water content (LWC). The RH could promote the active uptake of gaseous oxidation products into the aerosol liquid water (ALW), and showed a positive effect on SOA formation (Luo et al., 2019; White et al., 2014). However, an obvious inhibitory effect of RH on SOA formation was observed in the *m*-xylene-OH system (Zhang et al., 2019) and isoprene-NOx system (Jia and Xu, 2018). On the one hand, it has been proved that this inhibitory effect was caused by the suppression of condensation reactions and oligomers formation, and further affected the highly oxygenated organic molecules (HOMs) formation process (Carlton et al., 2009; Jia and Xu, 2018). On the other hand, the increase of RH could favour the exchange of OH into the particles, and more OH would react with SOA to produce small molecule products through fragmentation reactions and decreased SOA concentration (Liu et al., 2019b). All in all, the effect of RH on SOA formation has not been decided yet. What is certain, though, is that the RH could affect the chemical composition of SOA, hence change the physical nature (e.g., optical property) of the SOA. The effect of RH on the optical property of SOA did not get enough attention, and more studies should be conducted in further studies.

Toluene is one of the most important artificial VOCs in the troposphere (Ji et al., 2017; Lin et al., 2015). Toluene is an important precursor of SOA in the urban areas, and the toluene-derived SOA has important contribution to the light absorption of atmospheric particles (Laskin et al., 2015; Wang et al., 2019). However, the understanding of the absorbance of atmospheric particulates formed in the different environmental conditions is still limited. In this study, the toluene-derived SOA was formed through OH photooxidation in the presence or absence of NOx in dry and wet conditions using a 4 m^3 indoor smog chamber. In the present study, we investigated the mass concentration, chemical composition, optical absorption of toluene-derived SOA performed in the presence or absence of NOx in dry and wet conditions using a 4 m^3 indoor smog chamber through OH photooxidation. The UV-vis spectrum analysis was used to measure the optical property of toluene SOA. The chemical composition of SOA was detected with an Aerodyne aerosol mass spectrometer (AMS) online. The effect of RH on the SOA absorption could be explained by the alterations in functional groups of SOA. The results would help us to better understand the SOA formation mechanism and optical property in different RH conditions.

1. Materials and methods

A series of photochemical experiments with different RH conditions were carried out in a 4 m^3 smog chamber at East China Normal University. Briefly, 0.08 mm-thick FEP-Teflon film was used to construct the chamber. The particle wall loss rate constants are almost the same under different RH conditions. The average wall loss rate constant of the particles was 3.6×10^{-5} sec^{-1}, which was used to correct the measured SOA concentrations by the SMPS in this study. 50 UV-B lamps (TUV36W, Philips) with the peak wavelengths of 254 nm were used as the light source to form the OH radical in the chamber through the Hydrogen peroxide (H_2O_2) photolysis. In order to maximize and homogenize the interior UV-light intensity, mirror surface stainless steel was used as the interior wall of the chamber.

The purified dry air was used to clean the chamber for more than 18 hours before each experiment, and the concentration of NOx, SO_2, and particles was less than 1 ppbV, 1 ppbV, and 1 cm^{-3}, respectively. Zero air, which was generated by zero air supply (111-D3N, Thermo Scientific^{TM}, USA), was used to fill the chamber. A flow rate of zero air of 20 L/min was controlled by the mass flow controller (D088C/ZM, Beijing Sevenstar Electron Corporation) in the process of inflating. The RH of zero air is about 15%-20%, and it could provide dry conditions in the chamber directly. For the wet experiment, the zero air was humidified by bubbling the air through fritted glass in distilled water and RH>70%.

A measured amount of toluene (Sigma-Aldrich, analytically pure) and H_2O_2 solution (Sigma-Aldrich, 30 wt.% in H_2O) were injected into a Teflon bulb with the micro syringes, and vaporized from liquid to gas by the zero air, and finally blown into the chamber. NOx (Air Liquid Shanghai, 510 ppmV NO_2

Table 1 – Summary of experimental conditions in this study.

No.	Tolene (ppbV)	H_2O_2 (ppmV)	NO_2 (ppbV)	RH (%)	Temperature (°C)	SOA mass concentration[a] (μg/m^3)
Exp.1	790	1.98	–	25±1	20±1	622.9±15.3
Exp.2	790	1.98	–	79±1	20±1	486.4±15.5
Exp.3	790	1.98	62	26±1	20±1	434.5±14.9
Exp.4	790	1.98	63	79±1	20±1	400.3±15.9

RH: relative humidity.
[a] All the mass concentrations were wall-loss corrected.

in N_2) were directly introduced into the chamber for the required concentrations. Each experiment was performed without seed aerosols here. When the samples in the chamber were well combined, all the UV light lamps were turned on, and the photooxidation started. The experimental conditions for the toluene photooxidation were listed in **Table 1**.

The particle size distribution and volume concentration of toluene-derived SOA for each experiment were measured by the Scanning Mobility Particle Sizer (SMPS), which was composed of a differential mobility analyzer (DMA model 3081, TSI Inc., USA) for screening particulates with specific aerodynamic equivalent particle size and a condensation particle counters (CPC model 3776, TSI Inc., USA) for counting the number of the selected particles. The sheath gas and sample gas of SMPS were 3 and 0.3 L/min, respectively. The particle size scan range of the s was from 13.6 to 726.5 nm. The density of 1.4 g/cm^3 was used to convert the particle volume concentration measured by SMPS into mass concentration (Ng et al., 2007).

The chemical composition of toluene-derived SOA was characterized online through the Aerodyne high-resolution time-of-flight aerosol mass spectrometer (HR-ToF-AMS; Aerodyne Research Inc. USA). Before entering the AMS, the sample gas passed through a Nafion drying tube, and reduced the RH below 20%. Then, particles with the aerodynamic equivalent diameter below 1 μm were focused into a narrow beam by an aerodynamic lens at the injection port. The particles were ionized by electron collision (70 eV) after impacted on a flash vaporizer (600°C) and changed into vapours. The positively charged ions were separated in the ToF section, and then detected by quadrupole mass spectrometer with the scans across m/z 1 to 300. V-mode ($m/\Delta m = \sim 2000$), which has a higher signal-to-noise ratio, was used in the AMS ToF section. The composition-dependent collection efficiency (CE) was applied to the data based on Middlebrook et al. (Middlebrook et al., 2012). For mass concentration calculations, 1.1, 1.2, and 1.4 were used for the default relative ionization efficiency (RIE) values for nitrate, sulfate, and organic, respectively. The chemical composition data from AMS was analyzed through SQUIRREL 1.63B coupled with PIKA 1.23B in the Igor Pro (WaveMetrics, Inc., Portland, Oregon), which were available at http://cires1.colorado.edu/jimenezgroup /ToFAMSResources/ToFSoftware/index.html. Note that the elemental ratios (i.e., O/C, H/C, N/C) were calculated using the Aiken-Ambient method for comparison with previous studies (Aiken et al., 2008).

After the photooxidation reaction finished, the SOA was collected onto the 46.2 nm PTFE filter (Whatman^{TM}, UK) for offline analysis. The volume of sample gas was 3 m^3. The collected SOA sample was dissolved in 5 mL of methanol (HPLC grade, >99.8%) with 30 min of sonication to ensure all the SOA was completely dissolved. 0.2 μm PTFE syringe filters were used to remove the suspended insoluble particles. The absorption spectra of toluene-derived SOA under different conditions were presented by using a UV spectrophotometer (UV-3600, Shimadzu, Japan). The absorption was detected in the range of 200 to 800 nm with a resolution of 0.5 nm^{-1}. The mass absorption coefficient (MAC_λ, m^2/g) is a key parameter that describes the light-absorbing ability of the particles. The MAC_λ calculation is based on the SOA mass concentrations and light absorption coefficient. MAC_λ value is calculated using Eqs. (1) and (2):

$$Abs_\lambda = (A_\lambda - A_{700}) \times \frac{V_l}{V_a \times L} \times \ln(10) \quad (1)$$

$$MAC_\lambda = \frac{Abs_\lambda}{M} \quad (2)$$

Here A_λ is the light absorption intensity at a specific wavelength. A_{700} is the background value of light absorption intensity. V_l and V_a are the volume of methanol with dissolved particles and the sampled air, respectively. L is the optical path length. M represents the concentration of methanol-soluble organic carbon.

2. Results and discussion

2.1. *Effect of RH on SOA formation*

The SOA mass concentration was investigated under four conditions: dry and wet conditions in the absence of NOx, and dry and wet conditions in the presence of NOx. The wall-loss-corrected particle mass concentrations as a function of photooxidation reaction time are shown in **Fig. 1**.

A significantly negative effect of RH on SOA formation from toluene OH oxidation in the absence of NOx was observed. The maximum mass concentrations of toluene-derived SOA were 622.9±15.3 and 486.4±15.5 μg/m^3 in dry and wet condition, respectively. Similar results were also observed in the previous studies for the aromatic SOA formation (Cao and Jang, 2010; Tuet et al., 2017). Hinks et al. (2018) investigated the effect of RH on toluene SOA formation and found a significant reduction of SOA yield at high RH compared to that under low RH for

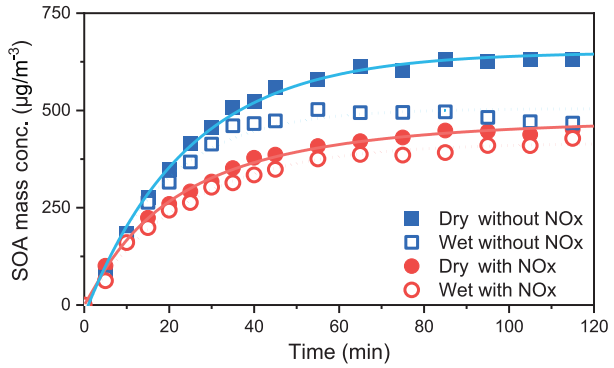

Fig. 1 – The evolution of SOA mass concentration at different RH and NOx conditions. All the SOA mass concentrations were corrected for the wall loss.

low-NOx conditions (Hinks et al., 2018). Zhang et al. (2019) also pointed the SOA yields for the aromatic-OH photooxidation system decreased by nearly 1 order when the RH increased from 24% to 74%-79% (Zhang et al., 2019). It has been proved that hemiacetal and peroxy hemiacetal oligomers are the major chemical components of toluene derived aerosol (Sato et al., 2007). Water is involved as a by-product during the condensation reaction process and, thereby, oligomers formation was inhibited with the increasing RH conditions. The suppression of oligomers formation might be the key factor for the decreased SOA mass concentration. Besides, we cannot rule out the possibility that the mass loading of SOA was affected by the enhanced wall loss of more water-soluble compounds under high-RH conditions. The water-soluble products from toluene would be more efficiently absorbed by the wetted chamber walls at high RH conditions, and result in a stronger effect of RH on the SOA mass loading.

The lower toluene-derived SOA mass concentration was observed at elevated RH, regardless of the presence or absence of NOx. However, interestingly, when the experiments with NOx presence, the maximum mass concentration of toluene SOA was not significantly different under different RH conditions. When compared SOA mass concentration observed in the dry condition, the SOA formed at the wet condition decreased from 434.5±14.9 to 400.3±15.9 μg/m^3 as NOx introduced into the chamber. The SOA mass concentration decreased 9.8% as RH increased from dry to wet condition in the presence of NOx, but it decreased 29.1% in the absence of NOx. This result is well in line with the previous study of Hinks et al. (2018), which have similarly found that there was a much small difference in the maximum mass concentration achieved under < 2%, 40%, and 75% RH for the high-NOx experiments compared to the low-NOx experiments (Hinks et al., 2018). It is conceivable that less water-soluble products in the toluene-derived SOA were formed in the presence of NOx than those formed in the absence of NOx.

In both dry and wet conditions, The SOA mass concentration formed in the presence of NOx is lower than that in the absence of NOx. The production of low volatile compounds is likely to be inhibited in high-NOx experiments (Song et al., 2005; Yang et al., 2020). The previous study also reported that toluene SOA displayed higher mass concentration under low-NOx conditions and lower under high-NOx conditions (Ng et al., 2007). RO_2 are the important intermediates in the photooxidation process. The branching of RO_2 loss among different pathways has an important influence on the chemical composition of photooxidation products and thus on SOA formation (Zhao et al., 2018). The RO_2+RO_2/HO_2 reaction products are believed to be involved in SOA formation. The reaction rate constant of RO_2+RO_2 is 2.5 × 10^{-13} cm^3/(molecules·sec) (298 K), which is as much as 50 times slower than that of RO_2+NO (~9 × 10^{-12} cm^3/(molecules·sec) at 298 K) (Ziemann and Atkinson, 2012). In the presence of NOx, the reaction of RO_2 with NO was the major reaction pathway for RO_2 and led to the formation of RO radicals. RO could produce more volatile compounds through fragmentation and thus reduce SOA formation (Kirkby et al., 2016; Liu et al., 2019a, 2015b). With the increase of RH, the decrease ratio of mass concentration of toluene SOA formed without NOx is higher than that of toluene SOA formed with NOx. The decrease ratios were 30.3% and 17.7% for the dry and wet conditions, respectively. This result also pointed the inhibitor effect of NOx on toluene SOA formation would be weakened by the increasing RH.

The chemical properties of toluene SOA formed in the different conditions were detected by the AMS. The mass spectra of SOA formed under different RH conditions are shown in **Fig. 2**. The mass spectra were dominated by *m*/z 28, 29, 43, 44 for the organic fragments of CO^+, CHO^+, $C_2H_3O^+$, and CO_2^+, respectively. Both CO^+ and CO_2^+ originate from the fragmentation of organic acids, are the indicators of highly oxygenated organic aerosols (Alfarra et al., 2004; Ng et al., 2010). The CHO^+ and $C_2H_3O^+$ are the characteristic fragmentation ion of aldehydes and ketones (Ng et al., 2010; Chen et al., 2021). The fraction of the organic signal at *m*/z 44 is represented by f_{44}. In the experiments with the absence of NOx, f_{44} was persistently lower in wet condition, indicating that SOA formed under higher RH conditions were less oxidized, which was unfavourable to SOA formation. Seinfeld et al. (2001) pointed the promotion of partitioning of gas-phase products in wet condition would result in more insufficient oxidized gas-phase products were partitioned into the aerosol phase under higher RH conditions, and further reduced the oxidation state of SOA (Seinfeld et al., 2001). However, in the presence of NOx, f_{44} had no evident change between different RH conditions (0.089 in dry condition and 0.091 in wet condition). This might because the oxidation products in the presence of NOx are more volatile. These products with lower f_{44} are mainly participated in the gas-phase and more difficult to distribute into the particle-phase. This causes the decreasing trend of f_{44} with RH in the absence of NOx is not observed in the experiment with NOx presence.

The elemental analysis serves as a valuable tool to elucidate SOA chemical composition and SOA formation mechanisms (Heald et al., 2008; Chhabra et al., 2011). **Fig. 3** shows the ratios of O/C and N/C of toluene-derived SOA under different RH conditions. The changing trend of O/C was similar to that of f_{44} at different experiment conditions. O/C decreased with the increase of RH in the absence of NOx. It decreased from 0.897 in dry condition to 0.822 in wet condition. Although the O/C does not change obviously, a slight increase of O/C with RH could be observed in the presence of NOx. The O/C in-

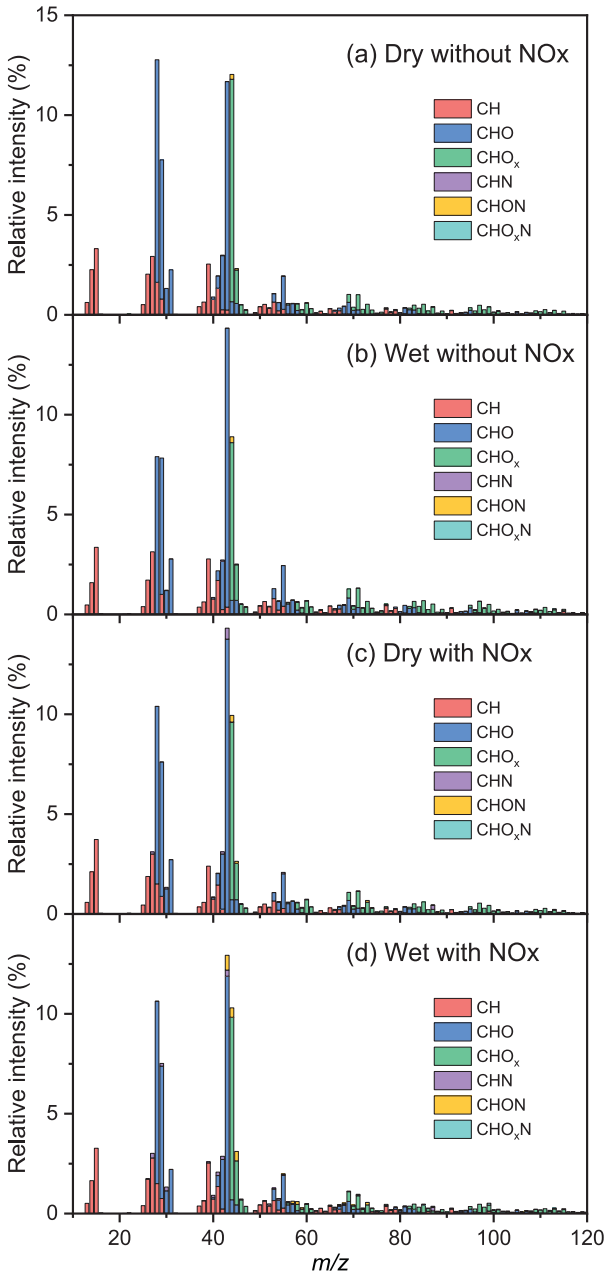

Fig. 2 – Mass spectra of SOA formed under different RH and NOx conditions. *m/z*: mass to charge ratio.

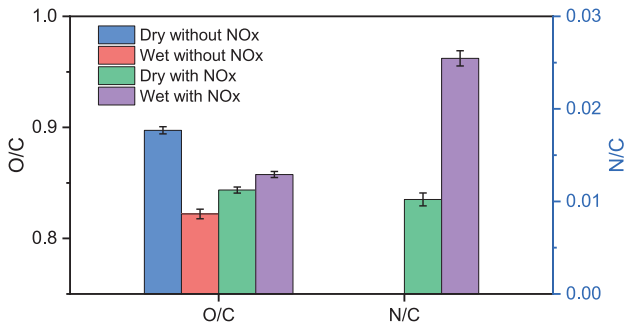

Fig. 3 – Ratios of O/C and N/C of toluene-derived SOA under different RH conditions.

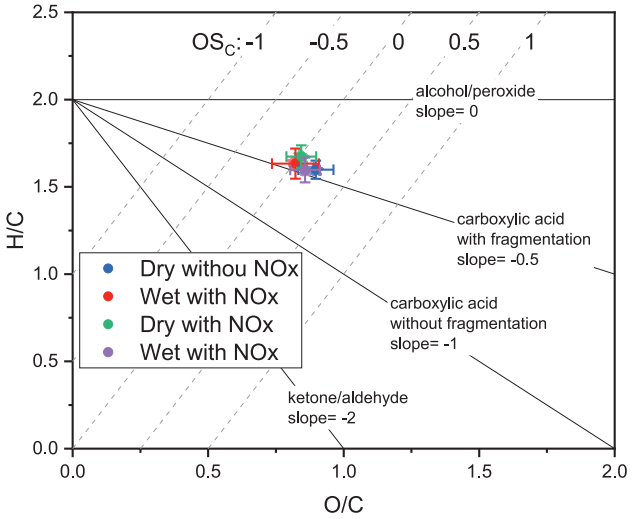

Fig. 4 – Van Krevelen diagram of toluene-derived SOA at different RH and NOx conditions.

creased from 0.844 in dry condition to 0.857 in wet condition in the presence of NOx. For the SOA formed in the presence of NOx, obvious nitrogen element was detected in the AMS results. The N/C was 0.010 in dry condition. The N/C value increased two and a half times to 0.025 in wet condition. It has been proved before that the presence of NOx could participate into the organic-phase in the form of nitro and nitrate groups through the atmospheric oxidation process. The formation of nitro and nitrate groups would provide extra Oxygen atoms for the oxidation products of toluene. We assume that, for the nitro and nitrate groups, each Nitrogen atom can carry two additional Oxygen atoms. If the increase of oxygen atoms caused by nitro and nitrate groups in the toluene-derived SOA were excluded in the presence of NOx, the O/C would decrease from 0.824 in dry condition to 0.807 in wet condition. Therefore, the increase of N/C with RH resulted in the growth of O/C in the condition with NOx presence.

The Van Krevelen diagram was developed to illustrate how elemental composition changes during SOA formation. The H/C and O/C of toluene SOA formed at different RH and NOx conditions were evaluated and displayed in the Van Krevelen diagram for the further investigation of the oxidation degree of SOA. The Van Krevelen diagram is shown in **Fig. 4**. Lines indicated slope of 0, −0.5, −1, −2 representing additions of alcohol or peroxide groups (OH or OOH), carboxylic acids (or simultaneous addition of carbonyl and alcohol groups) with fragmentation, carboxylic acids (or simultaneous addition of carbonyl and alcohol groups) without fragmentation, carbonyl groups (ketones and aldehydes), respectively (Heald et al., 2010).

The slope of the linear fit of H/C *vs.* O/C was used to illustrate the chemical processes involved in the evolution of SOA (Heald et al., 2010). The fitted slope for toluene SOA at different conditions is shown in **Fig. 5**. In the absence of NOx, the fitted slope of -0.59 ± 0.06 and -0.92 ± 0.03 were obtained for toluene SOA formed in the dry and wet conditions, respectively. The slopes indicated that the SOA formed from photooxidation of toluene was mainly composed of the carboxylic acid with frag-

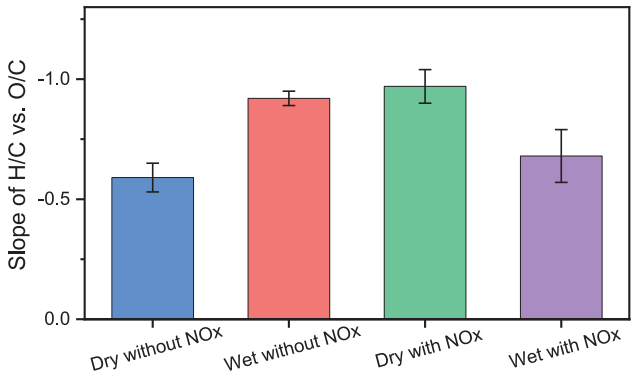

Fig. 5 – Slope of the linear fit of H/C *vs.* O/C of toluene-derived SOA at different RH and NOx conditions in the Van Krevelen diagram.

mentation in the dry condition and without fragmentation in the wet condition. Carboxylic acid formed with fragmentation has smaller molecular weight and has higher volatility than that without fragmentation. The less relatively volatile substance is distributed into the particle-phase in the wet condition than that in the dry condition, indicated that the SOA formation was inhibited as RH increased in the photooxidation of toluene. However, in the presence of NOx, the fitted slope of -0.97 ± 0.07 and -0.68 ± 0.11 were obtained for toluene SOA formed in the dry and wet conditions, respectively. The slope of the linear fit of H/C *vs.* O/C in the presence and absence of NOx also presented the opposite trend with RH. These results indicated that NOx not only played a significant effect on the SOA formation, but also changed the effect of RH on the toluene-derived SOA chemistry composition.

2.2. *Effect of RH on SOA optical absorption*

Optical absorption is one of the important properties of SOA. The change of SOA optical absorption formed under different RH conditions was investigated in this section. The $MAC_{\lambda=365\ nm}$ of toluene SOA under different RH conditions are shown in **Fig. 6**. Whether in the dry or wet condition, $MAC_{\lambda=365\ nm}$ was higher in the presence of NOx than that in the absence of NOx, which indicated that the NO_2 could enhance the light-absorbing ability of SOA formed in the chamber. This result is in accordance with the previous studies (Xie et al., 2017; Lin et al., 2015). The effect of RH on the $MAC_{\lambda=365\ nm}$ absorbance in the presence or absence of NOx was different. The $MAC_{\lambda=365\ nm}$ value for the toluene SOA formed without NOx was almost unchanged between dry and wet conditions. The $MAC_{\lambda=365\ nm}$ is 0.157 and 0.153 m^2/g in the dry and wet conditions, respectively. This result indicated that the increased RH does not affect the optical absorption of SOA formed in the toluene/OH photooxidation system without NOx. Meanwhile, the $MAC_{\lambda=365\ nm}$ of toluene-derived SOA in the presence of NOx increased with RH. The $MAC_{\lambda=365\ nm}$ of SOA formed in dry condition is 0.281 m^2/g, and it increased to 0.404 m^2/g when the SOA formed in wet condition. The $MAC_{\lambda=365\ nm}$ value increased by 43.7% under wet condition compared with that under dry condition. The highest $MAC_{\lambda=365\ nm}$ value was observed in the wet condition with NOx presence. This result indicated that the presence of NOx and increasing RH synergistic enhanced the $MAC_{\lambda=365\ nm}$ of toluene SOA.

The formation of NOCs in the presence of NOx has been proved to contribute significantly to the light absorption of particles and responsible for the enhanced light absorption of the toluene-derived SOA (Liu et al., 2015b; Yan et al., 2020). The chemical properties of toluene SOA formed in the different conditions were detected by the AMS. Many Nitrogen-containing fragments were observed in toluene SOA from the AMS spectra when the NOx existed in the chamber. The dominated Nitrogen-containing fragments were observed at *m/z* 27 (CHN^+), 41 ($C_2H_3N^+$), 43 ($C_2H_5N^+$), 44 (CH_2ON^+), 45 (CH_3ON^+), and 73 ($C_3H_7ON^+$), respectively. In order to indicate the changes in chemical composition more intuitively, six fragment groups of CH, CHO, CHO_x, CHN, CHON, and CHO_xN were divided according to the atomic composition of the mass spectrum fragment observed in the AMS spectra. **Fig. 7** shows the difference in the mass spectra of toluene SOA formed in the presence of NOx at different RHs. The characteristic fragmentations of CHN, CHON, and CHO_xN families are derived from the NOCs (Liu et al., 2015b). However, the signal intensities of Nitrogen-containing fragments were weaker than those of the CH, CHO, and CHO_x families. It is important to note that some of the NOCs may fragment into ions that do not contain nitrogen atoms, and here were categorized into the groups of CH, CHO, CHO_x. Despite the concentration of CHN, CHON, and CHO_xN families in the SOA is very low (less than 6%), the concentration of NOCs should be higher than the concentration of the sum of CHN, CHON, and CHO_xN families shown in **Fig. 7**. The concentration of Nitrogen-containing fragments is 2.6% under dry condition. But in the wet condition, the concentration of Nitrogen-containing fragments increased to 5.9%. Obviously, the evolution of RH could promote the formation of NOCs. The concentration of nitrogen-containing fragments increased by 123% from dry condition to wet condition, which is much higher than the increased ratio of $MAC_{\lambda=365\ nm}$ with the evolution of RH.

Fig. 7 shows that the change of the relative proportion of different kinds of NOCs is obviously different. Compared with the dry condition, the ratio of intensity of CHON and CHO_xN observed in the wet condition increased from 0.5% to 1.1% and from 0.7% to 2.6%, respectively. The proportion of CHN family in SOA also increased from 1.3% under the dry condition to 2.2% under wet condition. The proportion of CHN family experienced a sixty-nine per cent increase in wet condition as compared to that at dry condition, which was consisted with the increasing ratio of $MAC_{\lambda=365\ nm}$. However, the proportion of CHN in the Nitrogen-containing fragments in the SOA was decreased from 52% under the dry condition to 38% under wet condition. The organonitrates, one of the important Nitrogen-containing organic components, widely exist in the atmosphere (Li et al., 2018). C-O-N is the basic structure of organonitrogen molecules, where the Nitrogen atom can only directly connect to the oxygen atom. Hence, CHN family, in which a nitrogen atom is bonded directly to a carbon atom, could not be fragmented from organonitrates. The nitro compounds should be the source of CHN family fragmentations, and responsible for the increased value of $MAC_{\lambda=365\ nm}$ of toluene-derived SOA. Some nitro compounds, e.g., 4-nitro-

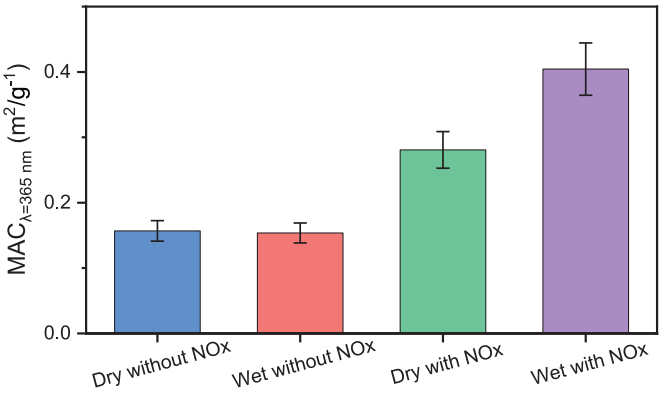

Fig. 6 – The value of $MAC_{\lambda=365\ nm}$ of toluene SOA formed at different RH and NOx conditions.

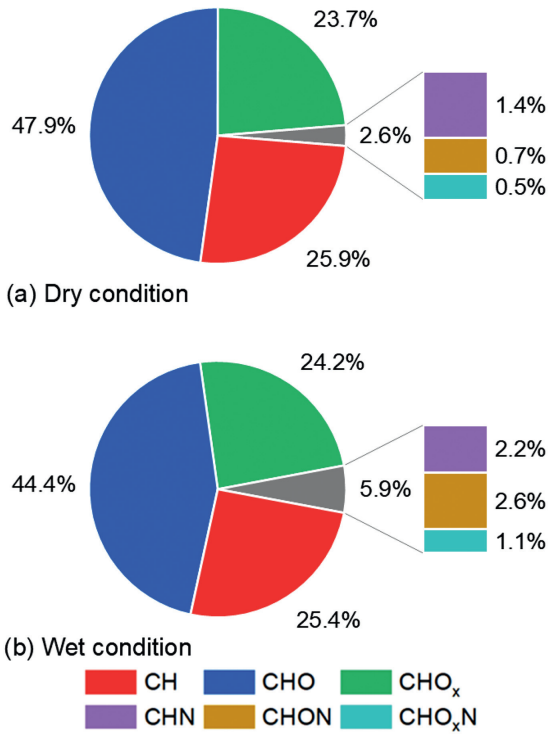

Fig. 7 – Chemical composition of toluene-derived SOA in the presence of NOx under (a) dry and (b) wet conditions measured by the Aerodyne high-resolution time-of-flight aerosol mass spectrometer (HR-ToF-AMS).

o-cresols, 4,6-dinitro-o-cresol, and 3-methyl-5-nitrobenzene-1,2-diol, could be formed in the toluene/NOx photooxidation system (Jang and Kamens, 2001; Wang et al., 2019). Future studies are necessary to quantify the concentration of these nitro compounds formed at different RH conditions via a liquid chromatography-electrospray ionization multi-stage mass spectrometry (LC-ESI-MS).

Although the proportion of CHN, CHON, CHO_xN families increased from dry to wet conditions. CHN family accounted for half of the Nitrogen-containing fragments in the dry condition, which meant that the nitro compounds were the main component of NOCs in the dry condition. The CHON and CHO_xN family fragmentations were the characteristic fragmentations of organonitrates. The proportion of CHON and CHO_xN increased from 50% to more than 62% from dry to wet condition, and become the main component of NOCs in the wet condition, suggesting the promotion of RH on organonitrates formation is more efficient than that on nitro compounds, and the increased RH promoted the proportion of organonitrates in NOCs and SOA.

3. Conclusions

In this study, mass concentration, chemical composition, and optical operation of toluene-derived SOA in dry and wet conditions were compared in the presence or absence of NOx. We found that both RH and NOx could suppress the formation of toluene-derived SOA. The SOA maximum mass concentration at wet condition to that in dry condition decreased from 622.9±15.3 to 486.4±15.5 μg/m^3, and decreased from 434.5±14.9 to 400.3±15.9 μg/m^3 with NOx absence and presence, respectively. The inhibitor effects of NOx and RH on toluene SOA formation were weakened by each other. The changing trends of SOA optical property are not consistent under different NOx conditions. In the absence of NOx, the $MAC_{\lambda=365\ nm}$ of toluene-derived SOA was almost unchanged with increasing RH. Meanwhile, the $MAC_{\lambda=365\ nm}$ of SOA formed in wet condition (0.404 m^2/g) increased 43.7% to that in dry conditions (0.28 m^2/g) with NOx presence. HR-ToF-AMS results showed that the wet condition significantly promoted the formation of NOCs. The concentration of Nitrogen-containing fragments is 2.6% in dry condition, and it increased to 5.9% in wet condition. The ratio of the CHN family showed a robust linear correlation with $MAC_{\lambda=365\ nm}$, suggesting a dominant contribution of nitro-aromatic compounds to the light absorption of toluene-derived SOA through the OH-photooxidation.

NOx is one of the most common pollutants in the atmospheric environment, and plays an important role in SOA formation. But the effect of NOx on SOA formation also influenced by other environmental factors. In this work, we revealed a synergy effect of NOx and RH on toluene-derived SOA concentration, chemical composition, and optical property. Due to the large latitude span in China, there is a great

difference in environmental humidity between the north and south regions. Our work will help in further understanding the different effects of NOx emission reduction on SOA in different regions.

In this study, the synergy effect of RH and NOx on SOA formation was studied qualitatively. The further chamber experiments should be investigated to clarify the synergy effect of RH and NOx on SOA formation quantitatively and provide parameterization scheme for improving air quality model.

Acknowledgments

This work was financially supported by National Key R&D Plan programs (No. 2017YFC0212703), the National Natural Science Foundation of China (Nos. 41773117, 42005088), the China Postdoctoral Science Foundation (No. 2019M661427), Fundamental Research Funds for the Central Universities, Director's Fund of Key Laboratory of Geographic Information Science (Ministry of Education), East China Normal University (No. KLGIS2021C02), and ECNU Happiness Flower Program.

REFERENCES

Aiken, A. C., DeCarlo, P. F., Kroll, J. H., Worsnop, D. R., Huffman, J. A., Docherty, K. S., et al., 2008. O/C and OM/OC ratios of primary, secondary, and ambient organic aerosols with high-resolution time-of-flight aerosol mass spectrometry. Environ. Sci. Technol. 42, 4478–4485.

Alfarra, M.R., Coe, H., Allan, J.D., Bower, K.N., Boudries, H., Canagaratna, M.R., et al., 2004. Characterization of urban and rural organic particulate in the lower Fraser valley using two aerodyne aerosol mass spectrometers. Atmos. Environ. 38, 5745–5758.

Cao, G., Jang, M., 2010. An SOA model for toluene oxidation in the presence of inorganic aerosols. Environ. Sci. Technol. 44, 727–733.

Carlton, A.G., Wiedinmyer, C., Kroll, J.H. , 2009. A review of secondary organic aerosol (SOA) formation from isoprene. Atmos. Chem. Phys. 9, 4987–5005.

Chen, T., Chu, B., Ma, Q., Zhang, P., Liu, J., He, H. , 2021. Effect of relative humidity on SOA formation from aromatic hydrocarbons: Implications from the evolution of gas- and particle-phase species. Sci. Total. Environ. 773, 145015.

Chhabra, P.S., Ng, N.L., Canagaratna, M.R., Corrigan, A.L., Russell, L.M., Worsnop, D.R., et al. , 2011. Elemental composition and oxidation of chamber organic aerosol. Atmos. Chem. Phys. 11, 8827–8845.

Chow, K.S., Huang, X.H.H., Yu, J.Z. , 2016. Quantification of nitroaromatic compounds in atmospheric fine particulate matter in Hong Kong over 3 years: field measurement evidence for secondary formation derived from biomass burning emissions. Environ. Chem. 13, 665–673.

George, C., Ammann, M., D'Anna, B., Donaldson, D.J., Nizkorodov, S.A. , 2015. Heterogeneous photochemistry in the atmosphere. Chem. Rev. 115, 4218–4258.

Han, T.T., Ma, Z.Q., Li, Y.R., Pu, W.W., Qiao, L., Shang, J., et al., 2021. Real-time measurements of aromatic hydrocarbons at a regional background station in North China: Seasonal variations, meteorological effects, and source implications. Atmos. Res. 250, 105371 ARTN 105371.

Heald, C.L., Goldstein, A.H., Allan, J.D., Aiken, A.C., Apel, E., Atlas, E.L., et al. , 2008. Total observed organic carbon (TOOC) in the atmosphere: a synthesis of North American observations. Atmos. Chem. Phys. 8, 2007–2025.

Heald, C.L., Kroll, J.H., Jimenez, J.L., Docherty, K.S., DeCarlo, P.F., Aiken, A.C., et al., 2010. A simplified description of the evolution of organic aerosol composition in the atmosphere. Geophys. Res. Lett. 37, L08803 Artn L08803.

Hinks, M.L., Montoya-Aguilera, J., Ellison, L., Lin, P., Laskin, A., Laskin, J., et al. , 2018. Effect of relative humidity on the composition of secondary organic aerosol from the oxidation of toluene. Atmos. Chem. Phys. 18, 1643–1652.

Jang, M., Kamens, R.M. , 2001. Characterization of secondary aerosol from the photooxidation of toluene in the presence of NOx and 1-propene. Environ. Sci. Technol. 35, 3626–3639.

Ji, Y., Zhao, J., Terazono, H., Misawa, K., Levitt, N.P., Li, Y., et al. , 2017. Reassessing the atmospheric oxidation mechanism of toluene. Proc. Natl. Acad. Sci. USA 114, 8169–8174.

Jia, L., Xu, Y. , 2018. Different roles of water in secondary organic aerosol formation from toluene and isoprene. Atmos. Chem. Phys. 18, 8137–8154.

Jo, D.S., Park, R.J., Lee, S., Kim, S.W., Zhang, X. , 2016. A global simulation of brown carbon: implications for photochemistry and direct radiative effect. Atmos. Chem. Phys. 16, 3413–3432.

Kirkby, J., Duplissy, J., Sengupta, K., Frege, C., Gordon, H., Williamson, C., et al. , 2016. Ion-induced nucleation of pure biogenic particles. Nature 533, 521–526.

Laskin, A., Laskin, J., Nizkorodov, S.A. , 2015. Chemistry of atmospheric brown carbon. Chem. Rev. 115, 4335–4382.

Li, R., Wang, X.F., Gu, R.R., Lu, C.Y., Zhu, F.P., Xue, L.K., et al. , 2018. Identification and semi-quantification of biogenic organic nitrates in ambient particulate matters by UHPLC/ESI-MS. Atmos. Environ. 176, 140–147.

Lin, P., Liu, J., Shilling, J.E., Kathmann, S.M., Laskin, J., Laskin, A. , 2015. Molecular characterization of brown carbon (BrC) chromophores in secondary organic aerosol generated from photo-oxidation of toluene. Phys. Chem. Chem. Phys. 17, 23312–23325.

Liu, P.F., Abdelmalki, N., Hung, H.M., Wang, Y., Brune, W.H., Martin, S.T., 2015a. Ultraviolet and visible complex refractive indices of secondary organic material produced by photooxidation of the aromatic compounds toluene and m-xylene. Atmos. Chem. Phys. 15, 1435–1446.

Liu, S.J., Jiang, X.T., Tsona, N.T., Lv, C., Du, L., 2019a. Effects of NOx, SO_2 and RH on the SOA formation from cyclohexene photooxidation. Chemosphere 216, 794–804.

Liu, S.J., Tsona, N.T., Zhang, Q., Jia, L., Xu, Y.F., Du, L., 2019b. Influence of relative humidity on cyclohexene SOA formation from OH photooxidation. Chemosphere 231, 478–486.

Liu, Y.C., Liggio, J., Staebler, R., Li, S.M., 2015b. Reactive uptake of ammonia to secondary organic aerosols: Kinetics of organonitrogen formation. Atmos. Chem. Phys. 15, 13569–13584.

Luo, H., Jia, L., Wan, Q., An, T.C., Wang, Y.J., 2019. Role of liquid water in the formation of O_3 and SOA particles from 1,2,3-trimethylbenzene. Atmos. Environ. 217, 116955 ARTN 116955.

Mehra, A., Wang, Y.W., Krechmer, J.E., Lambe, A., Majluf, F., Morris, M.A., et al. , 2020. Evaluation of the chemical composition of gas- and particle-phase products of aromatic oxidation. Atmos. Chem. Phys. 20, 9783–9803.

Middlebrook, A.M., Bahreini, R., Jimenez, J.L., Canagaratna, M.R. , 2012. Evaluation of composition-dependent collection efficiencies for the aerodyne aerosol mass spectrometer using field data. Aerosol Sci. Tech. 46, 258–271.

Moise, T., Flores, J.M., Rudich, Y. , 2015. Optical properties of secondary organic aerosols and their changes by chemical processes. Chem. Rev. 115, 4400–4439.

Ng, N.L., Kroll, J.H., Chan, A.W.H., Chhabra, P.S., Flagan, R.C., Seinfeld, J.H. , 2007. Secondary organic aerosol formation from m-xylene, toluene, and benzene. Atmos. Chem. Phys. 7, 3909–3922.

Ng, N.L., Canagaratna, M.R., Zhang, Q., Jimenez, J.L., Tian, J., Ulbrich, I.M., et al. , 2010. Organic aerosol components observed in Northern Hemispheric datasets from aerosol mass spectrometry. Atmos. Chem. Phys. 10, 4625–4641.

Paciga, A.L., Riipinen, I., Pandis, S.N. , 2014. Effect of ammonia on the volatility of organic diacids. Environ. Sci. Technol. 48, 13769–13775.

Priestley, M., Bannan, T.J., Le Breton, M., Worrall, S.D., Kang, S., Pullinen, I., et al. , 2021. Chemical characterisation of benzene oxidation products under high- and low-NOx conditions using chemical ionisation mass spectrometry. Atmos. Chem. Phys. 21, 3473–3490.

Pullinen, I., Schmitt, S., Kang, S., Sarrafzadeh, M., Schlag, P., Andres, S., et al. , 2020. Impact of NOx on secondary organic aerosol (SOA) formation from alpha-pinene and beta-pinene photooxidation: the role of highly oxygenated organic nitrates. Atmos. Chem. Phys. 20, 10125–10147.

Sarrafzadeh, M., Wildt, J., Pullinen, I., Springer, M., Kleist, E., Tillmann, R., et al. , 2016. Impact of NOx and OH on secondary organic aerosol formation from beta-pinene photooxidation. Atmos. Chem. Phys. 16, 11237–11248.

Sato, K., Hatakeyama, S., Imamura, T. , 2007. Secondary organic aerosol formation during the photooxidation of toluene: NOx dependence of chemical composition. J. Phys. Chem. A 111, 9796–9808.

Schwantes, R.H., Charan, S.M., Bates, K.H., Huang, Y., Nguyen, T.B., Mai, H., et al. , 2019. Low-volatility compounds contribute significantly to isoprene secondary organic aerosol (SOA) under high-NOx conditions. Atmos. Chem. Phys. 19, 7255–7278.

Seinfeld, J.H., Erdakos, G.B., Asher, W.E., Pankow, J.F. , 2001. Modeling the formation of secondary organic aerosol (SOA). 2. The predicted effects of relative humidity on aerosol formation in the alpha-pinene-, beta-pinene-, sabinene-, delta 3-carene-, and cyclohexene-ozone systems. Environ. Sci. Technol. 35, 1806–1817 +.

Song, C., Na, K., Cocker 3rd, D.R. , 2005. Impact of the hydrocarbon to NOx ratio on secondary organic aerosol formation. Environ. Sci. Technol. 39, 3143–3149.

Surratt, J.D., Murphy, S.M., Kroll, J.H., Ng, N.L., Hildebrandt, L., Sorooshian, A., et al. , 2006. Chemical composition of secondary organic aerosol formed from the photooxidation of isoprene. J. Phys. Chem. A 110, 9665–9690.

Tuet, W.Y., Chen, Y., Xu, L., Fok, S., Gao, D., Weber, R.J., et al. , 2017. Chemical oxidative potential of secondary organic aerosol (SOA) generated from the photooxidation of biogenic and anthropogenic volatile organic compounds. Atmos. Chem. Phys. 17, 839–853.

Wang, Y., Hu, M., Wang, Y., Zheng, J., Shang, D., Yang, Y., Liu, Y., et al., 2019. The formation of nitro-aromatic compounds under high NOx and anthropogenic VOC conditions in urban Beijing, China. Atmos. Chem. Phys. 19, 7649–7665.

White, S.J., Jamie, I.M., Angove, D.E. , 2014. Chemical characterisation of semi-volatile and aerosol compounds from the photooxidation of toluene and NOx. Atmos. Environ. 83, 237–244.

Xie, M., Chen, X., Hays, M.D., Lewandowski, M., Offenberg, J., Kleindienst, T.E., et al. , 2017. Light absorption of secondary organic aerosol: Composition and contribution of nitroaromatic compounds. Environ. Sci. Technol. 51, 11607–11616.

Yan, C., Zheng, M., Desyaterik, Y., Sullivan, A., Wu, Y.S., Collett, J.L. , 2020. Molecular characterization of water-soluble brown carbon chromophores in Beijing. China, J. Geophys. Res.-Atmos. 125, 18.

Yang, Z., Tsona, N.T., Li, J., Wang, S., Xu, L., You, B., et al. , 2020. Effects of NOx and SO_2 on the secondary organic aerosol formation from the photooxidation of 1,3,5-trimethylbenzene: A new source of organosulfates. Environ. Pollut. 264, 114742.

Zhang, Q., Xu, Y., Jia, L. , 2019. Secondary organic aerosol formation from OH-initiated oxidation of m-xylene: effects of relative humidity on yield and chemical composition. Atmos. Chem. Phys. 19, 15007–15021.

Zhang, R., Wang, G., Guo, S., Zamora, M.L., Ying, Q., Lin, Y., et al. , 2015. Formation of urban fine particulate matter. Chem. Rev. 115, 3803–3855.

Zhao, D.F., Schmitt, S.H., Wang, M.J., Acir, I.H., Tillmann, R., Tan, Z.F., et al. , 2018. Effects of NOx and SO_2 on the secondary organic aerosol formation from photooxidation of α-pinene and limonene. Atmos. Chem. Phys. 18, 1611–1628.

Ziemann, P.J., Atkinson, R. , 2012. Kinetics, products, and mechanisms of secondary organic aerosol formation. Chem. Soc. Rev. 41, 6582–6605.